ASSESSMENT OF PHYSIOLOGICAL AND PATHOLOGICAL REMODELLING IN ATHLETE'S HEART AND CARDIOMYOPATHIES USING CARDIAC MAGNETIC RESONANCE IMAGING

Doctoral Theses

Csilla Czimbalmos MD

Doctoral School of Basic and Translational Medicine
Semmelweis University

Supervisors: Hajnalka Vágó MD, PhD
Béla Merkely MD, DSc

Official reviewers:
Gergely Ágoston MD, PhD
Gergely Szabó MD, PhD

Head of the Final Examination Committee:
Zoltán Benyó MD, DSc

Members of the Final Examination Committee:
András Zsáry MD, PhD
Réka Faludi MD, PhD

Budapest
2020

INTRODUCTION

Cardiac remodelling is a compensatory process leading to functional and structural changes of the heart. The term cardiac remodelling was first used to describe maladaptive changes after myocardial infarction including scar formation, left ventricular dilation and geometrical changes with increasing spherical geometry. Similar changes in left and also right ventricular geometry may be present in cardiomyopathies. Moreover, certain geometrical and structural alterations observed in pathological cardiac remodelling may be also caused by physiological factors such as intensive and regular exercise. Cardiac magnetic resonance (CMR) imaging enables the assessment of the functional, morphological, mechanical and tissue specific changes in physiological and pathological cardiac remodelling.

AIMS

1. **Differentiation of pathological and physiological remodelling**

The first aim of our studies was to describe then compare characteristics of physiological and pathological remodelling in athletes as well in cardiomyopathy patients, and to investigate the clinical and CMR characteristics of elite athletes with hypertrophic cardiomyopathy (HCM) or arrhythmogenic right ventricular cardiomyopathy (ARVC). We aimed to establish CMR parameters and cut-off values which may help to differentiate pathological and physiological remodelling.

2. **Electro-anatomic and tissue characterization**

Second aim was to investigate structural and electrophysiological remodelling in dilated cardiomyopathy (DCM) patients by performing tissue characterization using CMR and electro-anatomic characterization using electro-anatomic mapping.

3. **Reverse remodelling assessment**

Third goal was to investigate reverse remodelling as an effect of cardiac resynchronization therapy in symptomatic heart failure patients despite optimal medical therapy with broad QRS and left bundle branch block (LBBB) morphology applying biventricular pacing during CMR examination. We also aimed to investigate the differences in the left ventricular function and mechanics between biventricular and asynchronous pacing modes.

METHODS

I. Study design and study population

1. Differentiation of pathological and physiological remodelling

This retrospective study was conducted in the Heart and Vascular Center of the Semmelweis Univesity. Healthy athletes, athletic and nonathletic HCM and ARVC patients were examined using CMR. Nonathletic HCM patients (n=194) with preserved left ventricular ejection fraction (LVEF ≥50%), and nonathletic ARVC patients with definite diagnoses based on the current Task Force Criteria (n=34) were enrolled. Ten additional athletes with HCM and eight athletes with ARVC were examined during training or competition period. Healthy athletes free of any cardiovascular diseases without electrocardiogram (ECG) abnormality suggesting structural heart disease were recruited. Highly trained healthy athletes with a minimum of 15 hours of training per week performing highly dynamic, and at least, moderate static sports served as a control group. The athletic cohort included canoe and kayak paddlers, water-polo players, rowers, handball players, speed skaters, swimmers, athletics, tennis players, cross country skiers, basketball players or cyclists.

2. Electro-anatomic and tissue characterization

This retrospective study was conducted in the Heart Center University of Leipzig. DCM patients (n=50, 58±15y, 39 male) who underwent radiofrequency catheter ablation (RFCA) of sustained ventricular tachycardia (VT), non-sustained VT (nsVT) or ventricular premature beats (VPB) and CMR scan (<30 days prior the ablation) were enrolled. The inclusion of the patients was based on the morphological appearance of a dilated left ventricle and reduced LVEF. Patients with significant coronary artery disease were excluded, and in case of VPB only patients without improvement of the LVEF after ablation were included. The CMR and electro-anatomic mapping (EAM) data were analysed by two blinded investigators, a third investigator was responsible for the spatial alignment of the EAM and CMR. An interrogation of the implantable cardioverter-defibrillator (ICD) devices and Holter ECGs were used to follow-up.

3. Reverse remodelling assessment

This prospective study was conducted in the Semmelweis University Heart and Vascular Center. Patients (n=13, 64±7y, 5 male) with CRT indication according to the current guidelines (symptomatic heart failure, LVEF ≤35%, New York Heart Association functional

class II-III on optimal medical therapy for at least 3 months), complete LBBB and broad QRS (>150 ms) were prospectively recruited. All patients were in sinus rhythm and normal atrioventricular conduction. Exclusion criteria were any contraindications of CMR examination or CRT implantation. Patients meeting all inclusion criteria and with no exclusion criteria underwent the implantation of a commercially available MRI conditional CRT-P (n=5) or CRT-D (n=8) device. Baseline CMR scan with contrast material was performed 1-14 days before CRT implantation, and follow-up non-contrast CMR scan was performed at 6 months ± 14 days after CRT implantation during biventricular pacing (DOO) and right atrial pacing (AOO). Changes of device parameters (e.g., impedance, thresholds, sensing and battery voltage) were recorded pre- and post CMR scan. ProBNP was measured and a 12-lead ECG was performed at baseline and follow-up. CRT response was defined as the followings: 1) super-response: decrease in LVESVi >30%, 2) response: decrease in LVESVi >15%, 3) non-response: decrease in LVESVi <15%.

II. Image aquisition and analysis

1. Differentiation of pathological and physiological remodelling

CMR examinations were conducted on a 1.5 T MR scanner (Achieva, Philips Medical Systems, Best, The Netherlands). For the assessment of cardiac dimensions and functions, at baseline retrospectively-gated, balanced steady-state free precession (bSSFP) segmented cine images were acquired in 2-chamber, 4-chamber and LV and RV outflow tract views. Short-axis images with full coverage of the left and right ventricle were obtained. Late gadolinium enhancement (LGE) imaging was performed. Contrast-enhanced images were acquired in the same views used for cine images 10–20 min after contrast administration.

In HCM patients and in the athletic control group images were evaluated using the Medis QMass 7.6 quantification software (Medis Medical Imaging Software, Leiden, The Netherlands). Endocardial and epicardial contour detection was performed manually on short axis cine images. Quantification of the left ventricular ejection fraction (LVEF), volumes (LVESV, LVEDV, LVSV) and myocardial mass (LVM) were performed using conventional (CQ) and threshold-based quantification method (TQ) as well. Left ventricular volumes and masses were standardized to body surface area (BSA). To further characterize the left ventricular hypertrophy and geometry, maximal diastolic wall thickness measurement was performed, and sport indices were derived using both conventional and threshold-based quantification method, such as left ventricular maximal end-diastolic wall thickness to end-

diastolic volume index ratio (EDWT(mm)/LVEDVi(ml/m^2)) and left ventricular mass to end-diastolic volume ratio (LVM(g)/LVEDV(ml)). Using threshold-based quantification TPM% ((TPM(g)/LVM(g)*100) was also established.

In ARVC patients and in the athletic control group quantification of left ventricular (LV) and right ventricular (RV) ejection fraction, volumes and myocardial mass were performed using conventional quantification method. Moreover, using feature tracking technique global LV and RV and regional strain analysis for the right ventricular free wall was performed. Peak systolic longitudinal strain and strain rate values of the basal, midventricular and apical free wall were established, and average and minimal strain values were calculated.

2. Electro-anatomic and tissue characterization

CMR examinations were conducted on a 1.5 T MR scanner (Philips Ingenia, The Netherlands). Balanced steady-state free precession (bSSFP) segmented cine images were acquired as described before. Three-dimensional, high-resolution LGE-CMR imaging was performed more than 10 min after the application of intravenous contrast (gadolinium- DTPA, 0.2 mmol/kg). For patients with ICDs or CRTs, we used multi-slice two-dimensional LGE employing the wideband technique. Image analysis was performed using IntelliSpace Portal 6, Philips Healthcare. LVEF, LVEDVi, LVESVi, LVSVi, and LVMi were evaluated based on short-axis images as described before. The presence or absence, pattern (subendocardial, mid-myocardial, subepicardial, transmural) and regional distribution of LGE areas were qualitatively assessed. Extent of the LGE and its volume were quantified by the full-width half maximum (FWHM) method.

Endo- and epicardial cardial detailed maps of the left ventricle were obtained during sinus rhythm or ventricular pacing using CARTO system (Biosense Webster Inc., Diamond Bar, CA) with a 3.5-mm open irrigated-tip catheter (Navistar Thermocool, Biosense Webster Inc.). Bipolar (bandpass filtered at 30 to 500 Hz) electrograms were recorded and analysed off-line. The perivalvular areas were excluded. The bipolar low-voltage areas were defined by the accepted thresholds for patients with ischaemic cardiomyopathy: 0.5–1.5 mV. The distribution of the low-voltage areas was described based on the AHA (American Heart Association) 17-segment model. The exit points of the VTs were defined as sites showing the best best pace-mapping sites (stimulus-QRS interval <80ms during pacing). First, we matched the CMR images with the EAM low-voltage areas defined using the standard bipolar threshold of 1.5mV. In terms of anatomical and electrical concordance, good agreement was defined if both EAM (<1.5mV) and CMR overlapped in all segments. Partially good

agreement was defined as an overlap between LGE and EAM (<1.5mV) in at least one corresponding segment or in anatomically adjacent segments. As a second step, if no agreement between LGE and EAM was observed, a manual adjustment of the EAM cut-off limits was performed to match with LGE areas. Finally, the surface areas of the redefined low-voltage areas were measured and the maximal surface area on the endocardial or the epicardial surface was compared with the amount of the LGE mass and its distribution.

The endpoint of acute success after ablation was non-inducibility of any sustained monomorphic VT with programmed ventricular stimulation. For patients with VPB, successful catheter ablation was defined as complete elimination of VPB.

3. Reverse remodelling assessment

CMR examinations were conducted on a 1.5 T MR scanner (Achieva, Philips Medical Systems, Best, The Netherlands). Retrospectively-gated, balanced steady-state free precession (bSSFP) segmented cine images were acquired in long- and short-axis views as described before. Additionally, high temporal resolution cine images with a temporal resolution of 50 phases per cardiac cycle were also acquired in 2-chamber, 4-chamber and 3-chamber views and in three short-axis slices (basal, mid, apical). At baseline, late gadolinium enhancement (LGE) imaging was also performed as described in the first project. At follow-up scans, whole body specific absorption rate (SAR) was restricted according to the prescription of the implanted devices, and to minimalize device-related artefacts, spoiled gradient echo (SGE) imaging was performed in CRT-D patients. Cardiac rhythm, blood pressure and pulse oximetry were monitored from the time of device programming until reprogramming using Invivo Precess 3160, Philips Medical Systems, Best, The Netherlands. Image analysis was performed using Medis Suite 3.0 software (Medis Medical Imaging Systems, Leiden, The Netherlands). Assessment of cardiac dimensions and functions were performed on short-axis cine image as described earlier. Additionally, remodelling parameters, such as 2D sphericity index (end-diastolic SA/LA diameter), 3D sphericity index (ESV/(4/3x π*(end-diastolic LA diameter/2)3) and relative wall thickness (RWT; 2xEDWT/end-diastolic LA diameter) were calculated. Quantitative deformation assessment was performed based on the manually endocardially contoured cine images using dedicated feature tracking quantification software (Medis Suite 3.0 QStrain, Leiden, The Netherlands). Global longitudinal (GLS), circumferential (GCS) and radial (GRS) left ventricular strain parameters were measured. Global left ventricular dyssynchrony was assessed by mechanical dispersion as the standard deviation of time to peak longitudinal (SD long TTP) and circumferential strain (SD circ

TTP) in 16 LV segments. Regional left ventricular dyssynchrony was assessed by the maximum differences in time between peak septal and lateral transversal displacement based on regional strain analysis. Allowing comparisons between patients with different heart rates, regional LV dyssynchrony is expressed in ms adjusted to a standard cardiac cycle length of 1000 ms. The presence and localization of LGE was evaluated on baseline scans.

Device interrogation was performed prior to CMR examination, in between different pacing modes and finally before patient discharge to record device parameters and verify system integrity. In order to achieve resynchronization therapy during image acquisition, the Medtronic devices were programmed manually according to Medtronic Field Technician's recommendations as these CRT devices are not able to perform biventricular pacing in MRI safe mode. Tachyarrhythmia detection and therapy was suspended in defibrillators. Atrial pacing was performed by SureScan mode (AOO), and base rate was the same as in the DOO pacing configuration in both groups. In case of Biotronik Intica 7 HF-T device, MRI safe mode was able to maintain resynchronization during CMR imaging. As MRI safe mode does not include AOO pacing as an option, pacing off option was used to mimic AOO mode.

III. Statistical analysis

All continuous variables are expressed as mean and standard deviation.

In the „Differentiation of pathological and physiological remodelling" project, when comparing HCM patients and athletes, between-groups comparisons were based on least-squares linear regression if normality assumptions were satisfied and median regression otherwise. Adjustment for age and heart frequency was applied.

When comparing ARVC patients and athletes, between-group comparisons were performed with the unpaired Student's t test or Mann–Whitney U-test where appropriate. For area under the curve (AUC), a value of 0.9–1.0 was considered excellent, 0.75–0.9 good, 0.6–0.75 moderate and 0.5–0.6 poor. Diagnostic accuracy of CMR parameters was evaluated using receiver operating characteristic (ROC) curve analysis. Cut-off values were set to maximize the proportion of subjects correctly classified.

In the second project, data structure has been tested with Shapiro–Wilk test for normal distribution. Groups were compared with test Student's t-test or Mann–Whitney U-test, and correlation analysis was also performed.

In the „Reverse remodelling" project, between–group comparisons were performed using paired Student's t-test or Wilcoxon test where appropriate. Pearson correlation coefficient was

used to measure of the strength of the association between LV dyssynchrony and remodelling parameters.

A p-value of ≤0.05 was considered statistically significant. Statistical analysis was performed using SPSS 20.0 (IBM, Armonk, NY, USA) and MedCalc software (version 17.9 Ostend, Belgium).

RESULTS

1. Differentiation of pathological and physiological remodelling

HCM and ahlete's heart

Fifteen percent of male HCM patients, 47.5% of male athletes, 19.8% of female HCM patients and 4.1% of female athletes were in the grey zone of borderline hypertrophy (EDWT 13-16 mm). Seventy-five percent of nonathletic HCM patients (n=194, 50.2±13.6y, 108 male) demonstrated LGE. None of the healthy athletes (n=150, 24.2±4.8 y, 101 male, male: 22.1±5.1 and female: 21.2±3.5 hours training/week) showed any LGE. In our study population LGE showed excellent positive predictive value (100%) but low negative predictive value (100%). Sport indices established using conventional (CQ) and threshold-based method (TQ) were also lower in athletes compared to HCM patients. CMR parameters in HCM patients and athletes established using the two quantification techniques are presented in **Table 1.**

	Male athlete (n=101) mean ± SD	**Male HCM (n=108)** mean ± SD	**Female athlete (n=49)** mean ± SD	**Female HCM (n=86)** mean ± SD
EDWT (mm)	12.6±1.3$^{*¥}$	22.1±5.4$^{\#}$	10.4±1.2$^{\#}$	19.7±5.2
Max/min EDWT	1.93±0.30$^{*¥}$	3.56±1.53	2.17±0.45$^{\#}$	3.86±1.63
Conventional quantification				
$LVEF_{CQ}$ (%)	57.4±4.36*	62.2±7.29$^{\#}$	58.4±4.51$^{\#}$	63.8±8.31
$LVESVi_{CQ}$ (ml/m^2)	52.6±9.60$^{*¥}$	35.2±10.1$^{\#}$	44.7±7.72$^{\#}$	29.1±9.67
$LVEDVi_{CQ}$ (ml/m^2)	123±14.0$^{*¥}$	91.6±16.7$^{\#}$	107±11.2$^{\#}$	79.9±13.8
$LVSVi_{CQ}$ (ml/m^2)	73.2±14.8$^{*¥}$	57.5±11.1$^{\#}$	62.5±6.80	50.7±9.96
$LVMi_{CQ}$ (g/m^2)	90.3±14.7$^{*¥}$	99.9±34.0$^{\#}$	65.9±10.7	76.9±22.9
Max EDWT/$LVEDVi_{CQ}$	0.10±0.02*	0.25±0.08	0.10±0.02$^{\#}$	0.25±0.07
$LVM_{CQ}/LVEDV_{CQ}$ (g/ml)	0.75±0.13$^{*¥}$	1.08±0.30	0.62±0.10$^{\#}$	0.97±0.25
Threshold-based quantification				
$LVEF_{TQ}$ (%)	65.7±4.9*	71.9±9.0$^{\#}$	65.7±6.4$^{\#}$	74.4±8.6
$LVESVi_{TQ}$ (ml/m^2)	34.9±7.4$^{*¥}$	18.6±6.5$^{\#}$	30.4±7.1$^{\#}$	14.5±6.3

$LVEDVi_{TQ}$ (ml/m^2)	101.0±12.1$^{*¥}$	66.2±11.1$^{\#}$	89.3±10.1$^{\#}$	57.0±11.1
$LVSVi_{TQ}$ (ml/m^2)	66.3±7.6$^{*¥}$	47.6±10.2$^{\#}$	58.8±7.1$^{\#}$	42.3±9.7
$LVMi_{TQ}$ (g/m^2)	113.0±16.8$^{*¥}$	126.0±40.5$^{\#}$	84.3±12.1$^{\#}$	101.0±27.8
Max $EDWT/LVEDVi_{TQ}$	0.13±0.02*	0.34±0.10	0.12±0.02$^{\#}$	0.36±0.12
$LVM_{TQ}/LVEDV_{TQ}$ (g/ml)	1.13±0.16$^{*¥}$	1.93±0.60	0.95±0.14$^{\#}$	1.83±0.56
TPM (g)	44.8±11.5$^{*¥}$	55.6±17.5$^{\#}$	32.1±7.7	40.5±11.1
TPMi (g/m^2)	21.4±4.8$^{*¥}$	27.4±8.6$^{\#}$	17.7±4.2	23.0±6.5
TPM% $=\frac{\text{TPM [g]}}{\text{LVM [g]}}$ x 100 (%)	19.0±3.7$^{*¥}$	22.1±4.6	21.1±4.7	23.1±4.1

Table 1: Left ventricular CMR parameters in the four subgroups evaluated using conventional (CQ) and threshold-based (TQ) quantification. *significantly different from male HCM, $^{\#}$significantly different from female HCM, $^{¥}$significantly different from female athletes

Although efficiency of EDWT/LVEDVi evaluated using TQ and CQ showed no significant difference, LVM/LVEDV evaluated using TQ performed significantly better than CQ in both males and females ($p< 0.001$). Sport indices showed high diagnostic accuracy also in the male subgroup with EDWT between 13-16 mm, LVM/LVEDV evaluated using TQ performed significantly better than CQ **(Figure 1)**.

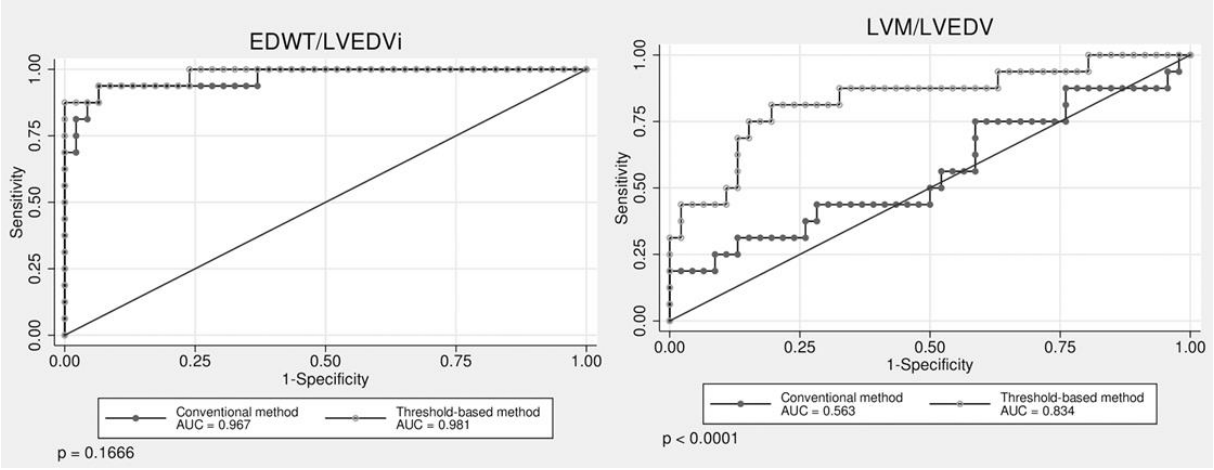

Figure 1: ROC curves visualizing correct identification of HCM among subgroup of individuals in the grey zone of hypertrophy (EDWT between 13–16 mm).

Cut-off values for sport indices are presented in **Table 2.** Despite the apparent gender-specific differences in cardiovascular sport adaptation, our cut-off values regarding sport indices are applicable in both males and females.

	Cut-off value	AUC	Sens	Spec	PPV	NPV	Correctly classified instances
Conventional quantification							
$EDWT/LVEDVi_{CQ}$ ($mm \times m^2/ml$)	>0.14	0.998	99.5	98.0	95.5	99.3	99.4
$LVM_{CQ}/LVEDV_{CQ}$ (g/ml)	>0.82	0.873	77.84	86.7	88.3	75.1	93.6
Threshold-based quantification							
$EDWT/LVEDVi_{TQ}$ ($mm \times m^2/ml$)	>0.17	0.999	99.0	99.3	99.5	98.7	99.4
$LVM_{TQ}/LVEDV_{TQ}$ (g/ml)	>1.27	0.948	89.2	91.3	93.0	86.7	94.4

Table 2: Cut-off values for optimised sensitivity and specificity of sport indices established using the two quantification method. PPV: Positive predictive value, NPV: negative predictive value.

In athletes with HCM (n=10, 9 male, 31±10 y, 14.4±6.5 hours training/week) 50% of the patients were int he grey zone of hypertrophy (EDWT 13-16 mm), and LGE was present in 40% in the hypertrophic regions and/or in the insertion points. According to our cut-off values $EDWT/LVEDVi_{CQ}$, $EDWT/LVEDVi_{TQ}$, $LVM_{CQ}/LVEDVi_{CQ}$ and $LVM_{TQ}/LVEDVi_{TQ}$ were in the pathological range in nine, nine, eight and 10 athletes with HCM, respectively.

ARVC and athletes's heart

Eighteen percent of the non-athlete ARVC patients (40.5±13.4 years, 40.5±13.4y, 22 male) had positive family history, 59% had recorded sustained ventricular tachycardia (VT) or ventricular fibrillation (VF), and aborted sudden cardiac death was reported in 12%. Average Task Force score (major = 2 points, minor = 1 point) was 4.9 points. Biventricular involvement was observed in 71%, LGE was present in 69%.

None of the healthy athletes (31.8±6.1 years; 22 male; 18.6±2.2 hours training/week) showed LGE or right ventricular wall motion abnormality. RVEDVi was in the proposed range of the major TFC (>110 ml/m^2 in males, >100 ml/m^2 in females) in all healthy male athletes and 83.3% of healthy female athletes. None of the athletes showed RVEF ≤45%, RVEF between 45 and 50% was observed in 5 cases (14.7%, three male and two female athletes).

Healthy athletes showed higher LVEDVi, LVSVi, LVMi, RVSVi and RVMi than non-athlete ARVC patients. No significant difference was found between athletes and non-athlete ARVC

patients regarding the RVEDVi. Both RVEF and LVEF were significantly lower in ARVC patients compared to healthy athletes. Right ventricular global longitudinal strain (RV GLS) was decreased in the ARVC group compared to athletes. Regional strain parameters (RV mid strain, RV mid strain rate, mean and minimum regional strain and strain rate) also showed significant difference between the two groups.

Establishing AUC values for the CMR parameters included in the current Task Force Criteria, RVEF showed good accuracy (AUC=0.830), whereas RVEDVi failed as a discriminator between ARVC and athlete's heart (AUC=0.599). AUC and cut-off values for CMR parameters are presented in **Table 3.**

	Cut-off value	**AUC**	**Sensitivity**	**Specificity**	**p**
CMR Task Force criteria					
RVEF	≤45.8	**0.830**	67.65	100.00	0.0001
RVEDVi	>150.8	0.599	29.41	94.12	NS
Global left and right ventricular strain values					
LV GLS	>-17.7	0.596	32.35	94.12	NS
LV GCS	>-22.5	0.643	38.24	100.00	0.0386
LV GRS	≤41.8	0.607	41.18	94.12	NS
RV GLS	>-20.1	0.726	50.00	97.06	0.0004
Regional strain values of the RV free wall					
RV basal strain	<-35.8	0.634	70.59	58.82	NS
RV mid strain	>-25.6	**0.767**	70.59	82.35	0.0001
RV apical strain	>-23.9	0.694	55.88	85.29	0.0042
RV average strain	>-29.4	**0.772**	73.53	76.47	0.0001
RV min strain	>-18.1	**0.786**	70.59	85.29	0.0001
RV basal strain rate	>-1.3	0.665	58.82	85.29	0.0195
RV mid strain rate	>-1,4	0.686	82.35	50.00	0.0045
RV apical strain rate	>-0.9	0.606	38.24	91.18	NS
RV average strain rate	>-1.13	0.665	52.94	88.24	0.0175
RV min strain rate	>0.8	0.702	55.88	82.35	0.0014

Table 3: Area under the ROC curves and cut-off values for optimised sensitivity and specificity of CMR parameters presented in the Task Force Criteria and global and regional strain parameters.

In the eight athletes with ARVC (27.6±3.3 y; 7 male; 18.9±4.6 hours training/week), applying the established cut-off values, RVEF was in the pathological range in only 3 athletes with ARVC. Half of the athletes with ARVC showed normal RV GLS. Regional longitudinal strain and strain rate of the RV mid free wall were in the pathological range in all eight athletes with ARVC **(Figure 2)**.

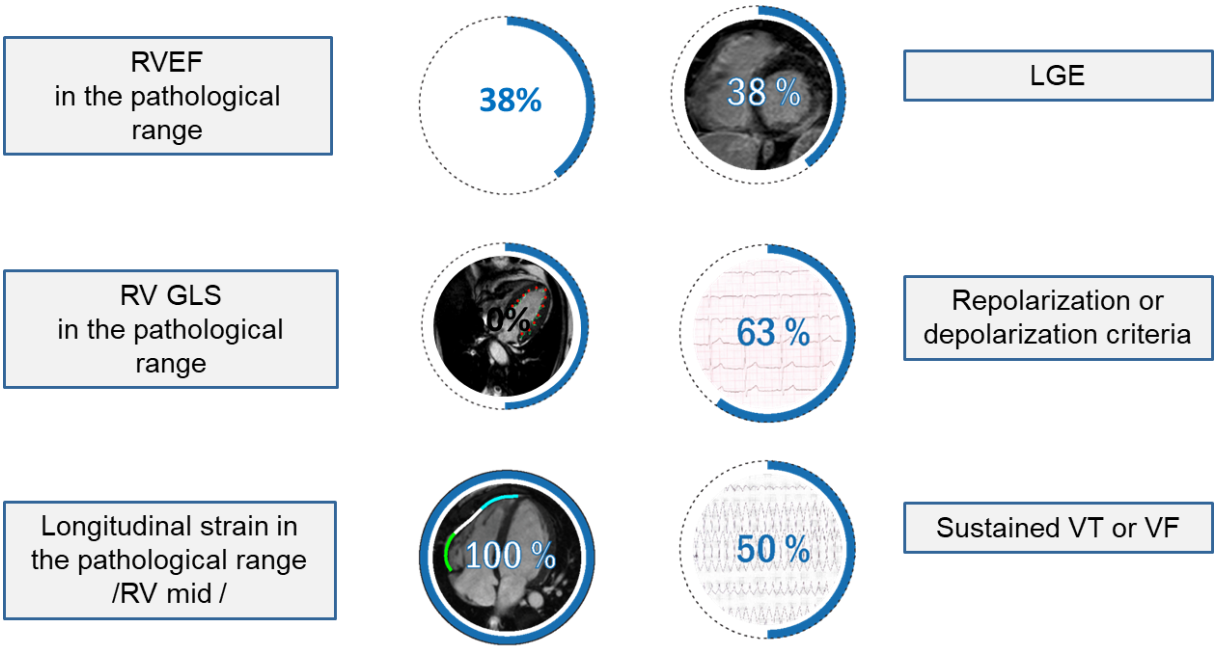

Figure 2: Clinical and CMR characteristics of athletes with ARVC.

2. Electro-anatomical and tissue characterization

Fifty DCM patients were identified who underwent RFCA (58± 15 years, 78% male, LVEF=35.5%± 12%; LVEDVi=121± 43ml/m^2). Of them, 21 (44%) patients received RFCA for sustained VT, 22 (42%) for pleomorphic VPB and nsVT, and seven (14%) for VPB from the left ventricular outflow tract or aortic cusps.

LGE was observed in 16 (32%) patients (LGE+). Epicardial LGE spreading to the mid-myocardial layers was observed in eight patients, only mid-myocardial LGE was observed in five patients, and endocardial to mid-myocardial LGE in three patients. LGE was detected in 63% patients with ICDs vs 13% patients without ICD ($p< 0.001$). Furthermore, LGE was observed in 71.4% of patients with sustained monomorphic VT, in 4.8% of patients with pleomorphic nsVT and in none of the patients with VPB originating from the LV summit ($p <0.0001$). The mean LGE mass was 10.6± 6.2 g and the mean LGE as a percentage of the LV

was 8.7%±5.4%. Twenty-three patients showed low-voltage area (<1.5 mV), 16 of them had RFCA due to sVT and seven due to nsVT or VPB.

In the 16 LGE+ patients, a good agreement between LGE and LVA (<1.5 mV) was observed in four (8%) patients, partially good agreement in nine (18%), and no agreement in three (6%) cases. Presence of low-voltage areas without any evidence of LGE was observed in seven (14%) patients. In 27 (54%) patients neither LGE nor low-voltage areas in EAM were detected.

Regarding VT exit sites, the best pace-mapping sites were observed in segments with LGE in 12 out of 16 patients. In two patients, the best pace-mapping sites were located in anatomically adjacent LGE segments, and in two patients—in segments without evidence of LGE in CMR. There was no significant correlation between the LGE extent and size of the low-voltage areas (<1.5 mV) in EAM (p=0.351).

In the LGE+ cases, the bipolar thresholds of low-voltage areas were individually adjusted in an attempt to match the localization and the size of the LGE. The median for the new bipolar threshold (Q1–Q3) was 1.5 (1.5–2.75) mV and the mean (SD) was 1.97±0.92 mV. The redefined bipolar EAM threshold showed a significant positive correlation with the LGE volume % (Pearson r=0.559).

Acute success was achieved in 12 out of 16 patients (75%). Recurrence of VT was observed in seven patients (44%) during one year of follow-up. The VT exits were found in areas with LGE in five out of seven patients with VT recurrence and in seven out of nine patients without VT recurrence. There was no difference in the surface of the low-voltage areas between patients with recurrence and without. In patients with VT recurrence, the LGE volume was significantly larger than in those without VT recurrence: 12%±5.76% vs 6.9%±3.4%; p=0.049.

3. Reverse remodelling assesment

A total of 13 patients (mean age 64±7 years, 38% male) were enrolled. CRT-D was implanted in 62%. Ten patients (77%) had non-ischaemic, one patient (8%) ischaemic and two patients (15%) had mixed aetiology based on the invasive coronary angiography and LGE pattern on CMR. Only one patient had prior acute myocardial infarction and PCI according to medical history. One patient showed no LGE, one patient had solely subendocardial LGE proving previous myocardial infarction, the two patients with mixed aetiology showed both subendocardial and midmyocardial LGE. Nine patients showed non-ischaemic LGE pattern: five of them had septal mid wall stripe pattern suggesting DCM, three patients showed focal

patchy midmyocardial LGE in the insertion points, and one patient had subepicardial LGE suggesting prior myocarditis.

The follow-up scanning time including both AOO and biventricular pacing was 46±6 minutes. During the CMR scan no supraventricular or ventricular arrhythmias were noted. Atrial fibrillation started ten minutes after the CMR scan in one patient. On the same day pharmacological cardioversion using amiodarone was successful. Follow-up interrogation one month later showed no atrial fibrillation episode. None of the patients showed pacemaker dysfunction. Pre- and post-MRI device interrogation yielded no significant changes (pacing threshold: atrial: 0.0±0.1 V, right and left ventricular lead: 0.0±0.0 V; change in pacing impedance: atrial: -21.2±23.9 Ω, RV: -0.4±17.3 Ω, LV lead: -29.2±32.6 Ω, and change in shock impedance in CRT-D patients: -0.4±2.3 Ω).

Left sided implantation was performed in all patients. Banding artefacts were present on bSSFP images in all patients with CRT-D. Therefore in CRT-D patients SGE cine images were also acquired achieving significant improvement of image quality. Precise analysis of SGE images was limited due to device artefacts in only two patients (three and two LV segments). Due to suboptimal image quality two patients were excluded from regional dyssynchrony analysis and one from global dyssynchrony and strain analysis. Device artefacts are presented in **Figure 3.**

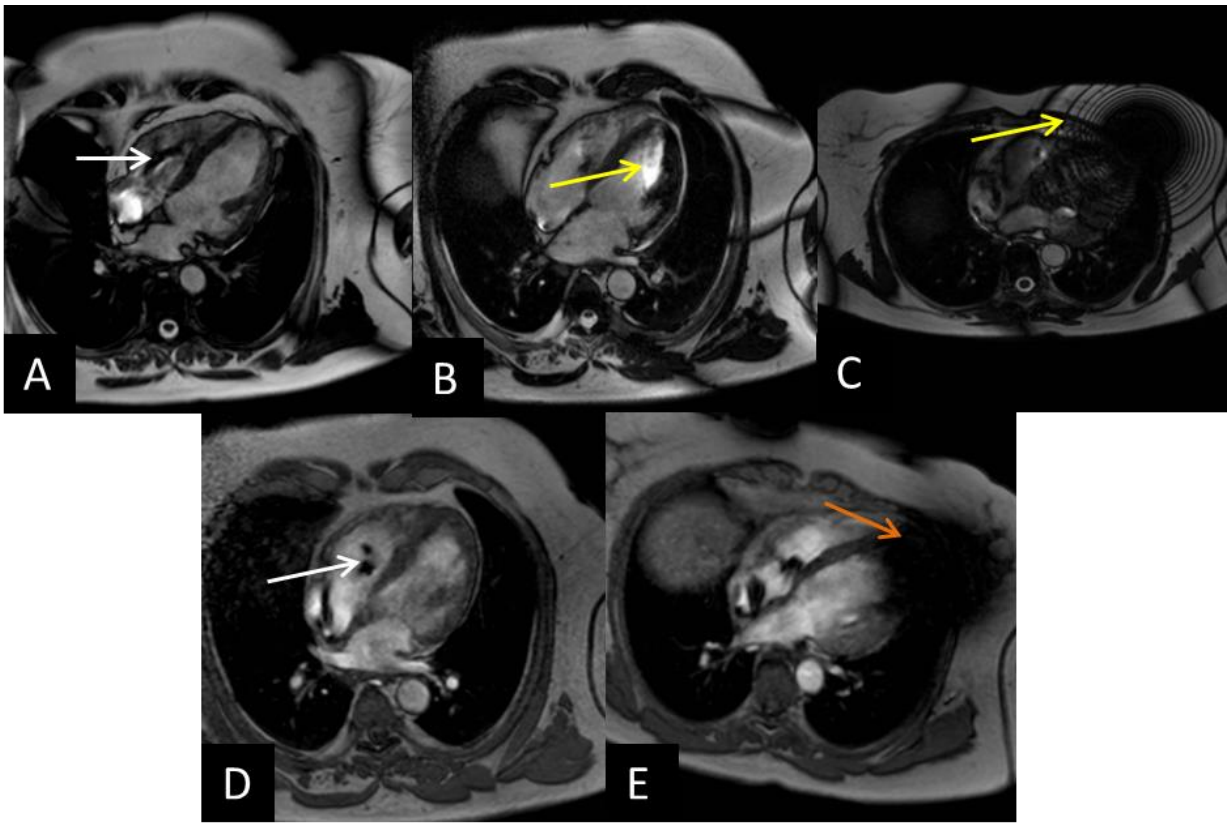

Figure 3: bSSFP (A-C) and SGE cine images (D,E) performed six months after CRT implantation. In case of CRT-P devices the generator related artefact on bSSFP images (yellow arrows) did not affect the heart, the lead related artefacts (white arrows) do not have any impact on the image analysis (A). In case of CRT-D devices generator related dark band off-resonance artefacts on bSSFP images are usually present (B,C). SGE images enable precise image analysis in majority of the cases (D), but suboptimal image quality could be present in some cases (E). bSSFP, balanced steady-state free precession; SGE, spoiled gradient echo

At 6-month follow-up two patients showed no symptomatic improvement (NYHA II), the conditions of 11 patients improved and were categorized in lower NYHA class **(Figure 4).** ProBNP levels (1186±863 vs 323±271 pg/ml, $p < 0.05$) and QRS width (165±9 vs 128±27, $p < 0.01$) decreased. Based on the decrease of LVESVi, 11 patients were classified as super responders, one patient as responder and one did not reach the 15% LVESVi decrease (ΔLVESVi 9%).

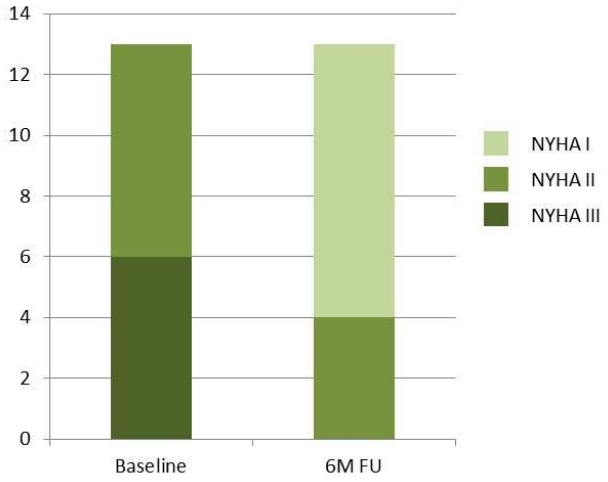

Figure 4: NYHA functional class at baseline and six months after CRT implantation. NYHA class improved in the vast majority of patients (85%) during the follow-up. NYHA, New York Heart Association Classification

Comparing baseline and follow-up CMR parameters measured during biventricular pacing significant differences were found; a marked increase in LVEF (27±7 vs 46±8%; p <0.001) and a decrease in LVEDVi (144±29 v 89±20 ml/m^2, p<0.001) and LVESVi (104±31 vs 49±16 ml/m^2, p <0.001) was detected. Left ventricular remodelling parameters such as relative wall thickness (0.33 ± 0.08 vs 0.45±0.09 p <0.001), 2D sphericity (0.70±0.11 vs 0.61±0.12 p <0.001) and 3D sphericity (0.44±0.12 vs 0.28 ± 0.11 p<0.01) indices showed a noticeable improvement.

Global left ventricular strain values also showed a significant improvement (GLS: -13.4±4.7 vs -17.3±3.0, p <005; GCS: -10.8±4.5 vs -21.3±4.9, p <0.001; GRS: 25.9±11.7 vs 38.8±10.8, p <0.01). The analysis of global dyssynchrony showed that circumferential mechanical dispersion decreased (20.5±5.5 vs 13.4±3.4, p <0.001), while the longitudinal mechanical dispersion did not show significant change.

Comparing regional dyssynchrony (defined by the maximum difference in time to peak septal and lateral transversal displacement) at baseline and at follow-up during biventricular pacing, it improved significantly (362±96 vs 104±66 ms, p <0.001). Decrease of regional dyssynchrony correlated with the decrease of LVESV (p <0.05, r =0.63) and with the increase of LVEF (p <0.05, r =0.66), and negative correlation between the decrease of regional dyssynchrony and RWT (p <0.05, r =-0.61) was found.

Comparing parameters measured at six months during biventricular and AOO pacing significant differences were found. We found that after switching off the biventricular pacing LVEF (45.7±7.6 vs 37.9±7.4%, p <0.001) and LVSVi immediately decreased (39.8±7.3 vs 33.1±8.7 ml/m^2, p <0.001), LVESVi immediately increased (49.0±15.5 vs 55.5±16.9 ml/m^2, p <0.001), and GCS deteriorated significantly (-21.3±4.9 vs -17.7±5.6, p <0.05). Mechanical dispersion (SD circ TTP 13.4±3.4 vs 17.0±4.4, p <0.05) and regional dyssynchrony increased (98±66 vs 335±148 ms, p <0.001) immediately **(Figure 5)**.

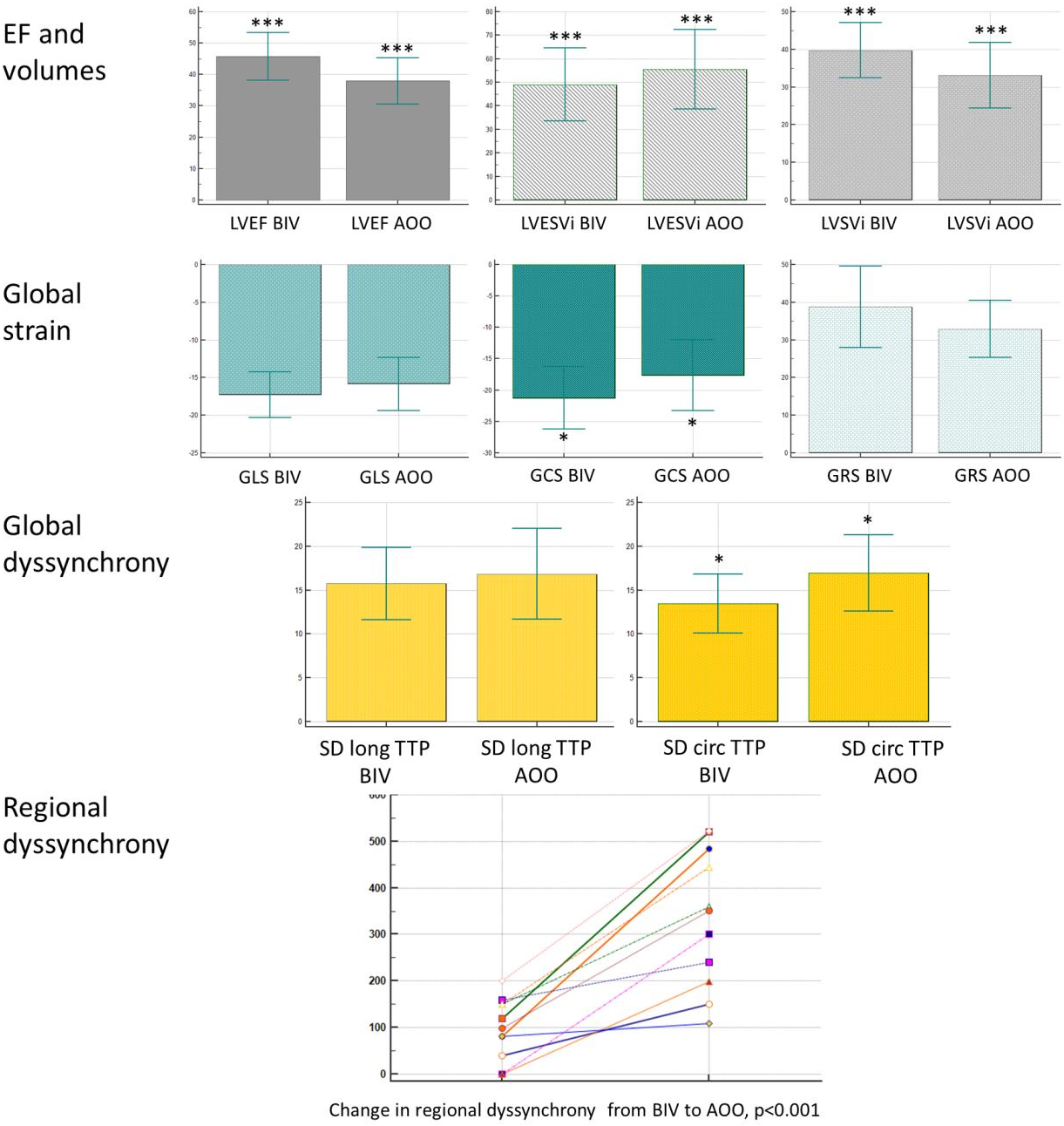

Figure 5: Comparison of CMR parameters at six months between biventricular and AOO pacing. Significance: * p <0.05, ** p <0.01, *** p <0.001.

CONCLUSION

Cardiac remodelling is a compensatory process leading to functional and structural changes of the heart including scar formation, left ventricular dilation and geometrical changes with increasing spherical geometry. Similar changes may be present in cardiomyopathies or in athletes with marked physiological remodelling.

As HCM and ARVC are leading causes of sudden cardiac death in young athletes, diagnosing these conditions in highly trained athletes is crucial. Novel CMR techniques may further improve the diagnostic accuracy and contribute to distinguish cardiomyopathies from marked physiological remodelling. We have first proven that sport indices such as EDWT/LVEDVi and LVM/LVEDV established using threshold based quantification may improve the diagnostic accuracy in athletes with suspected HCM. Our study has described first in the literature that CMR-based strain analysis is an important tool to distinguish ARVC from athlete's heart. CMR-based right ventricular regional strain values may help to identify ARVC even in highly trained athletes with preserved right ventricular ejection fraction.

Although it is known, that structural and electrophysiological remodelling are strongly related, to describe detailed information regarding tissue and electroanatomic characteristics of cardiomyopathy patients has been warranted. Based on our results, although only sub-optimal agreement could be found between the LGE and low-voltage areas, most VT exits were found in LGE areas in patients with sustained VT. Moreover, VT recurrence was influenced only by the LGE volume and none of the electroanatomic parameters. We have first proven that CMR imaging is a feasible and safe technique in CRT patients with resynchronization on, therefore precise assessment of reverse remodelling has become a clinical reality using biventricular pacing during CMR imaging. We have shown that in the absence of biventricular pacing (applying AOO pacing) immediate deterioration of function and mechanics occurs, therefore scanning with resynchronization on is crucial in this clinical setting.

Based on our results using different novel CMR techniques may improve the diagnostic accuracy in athletes with suspected cardiomyopathies. Moreover, it may contribute to our better understanding of structural and electrophysiological changes in cardiac remodelling and reverse remodelling as well.

PUBLICATIONS

Publications not related to dissertation (impact factor: 14.730)

1. Czimbalmos C, Csecs I, Dohy Z, Toth A, Suhai FI, Mussigbrodt A, Kiss O, Geller L, Merkely B, & Vago H (2019) Cardiac magnetic resonance based deformation imaging: role of feature tracking in athletes with suspected arrhythmogenic right ventricular cardiomyopathy. Int J Cardiovasc Imaging 35(3):529-538.
   ***** Authors contributed equally to this work
   IF: 1.860

2. Czimbalmos C, Csecs I, Toth A, Kiss O, Suhai FI, Sydo N, Dohy Z, Apor A, Merkely B, & Vago H (2019) The demanding grey zone: Sport indices by cardiac magnetic resonance imaging differentiate hypertrophic cardiomyopathy from athlete's heart. PLoS One 14(2):e0211624.
   ***** Authors contributed equally to this work
   IF: 2.766

3. Torri F, Czimbalmos C, Bertagnolli L, Oebel S, Bollmann A, Paetsch I, Jahnke C, Arya A, Merkely B, Hindricks G, & Dinov B (2019) Agreement between gadolinium-enhanced cardiac magnetic resonance and electro-anatomical maps in patients with non-ischaemic dilated cardiomyopathy and ventricular arrhythmias. Europace 21(9):1392-1399.
   IF: 5.047

4. Vago H, Czimbalmos C, Papp R, Szabo L, Toth A, Dohy Z, Csecs I, Suhai F, Kosztin A, Molnar L, Geller L, & Merkely B (2020) Biventricular pacing during cardiac magnetic resonance imaging. Europace 22(1):117-124.
   * Authors contributed equally to this work
   IF: 5.047

Publications not related to dissertation (impact factor: 31.193)

1. Csecs I, Yamaguchi T, Kheirkhahan M, Czimbalmos C, Fochler F, Kholmovski EG, Morris AK, Kaur G, Vago H, Merkely B, Chelu MG, Marrouche NF, & Wilson BD (2019) Left atrial functional and structural changes associated with ablation of atrial fibrillation - Cardiac magnetic resonance study. Int J Cardiol. In press.
   IF 3.471

2. Csecs I, Czimbalmos C, Toth A, Dohy Z, Suhai IF, Szabo L, Kovacs A, Lakatos B, Sydo N, Kheirkhahan M, Peritz D, Kiss O, Merkely B, & Vago H (2019) The impact of sex, age and training on biventricular cardiac adaptation in healthy adult and adolescent athletes: Cardiac magnetic resonance imaging study. Eur J Prev Cardiol:2047487319866019.4
   IF: 5.64

3. Mussigbrodt A, Czimbalmos C, Stauber A, Bertagnolli L, Bode K, Dagres N, Doring M, Richter S, Sommer P, Husser D, Bollmann A, Hindricks G, & Arya A (2019) Effect of Exercise on Outcome after Ventricular Tachycardia Ablation in Arrhythmogenic Right Ventricular Dysplasia/Cardiomyopathy. Int J Sports Med.
   IF: 2.132

4. Szucs A, Kiss AR, Suhai FI, Toth A, Gregor Z, Horvath M, Czimbalmos C, Csecs I, Dohy Z, Szabo LE, Merkely B, & Vago H (2019) The effect of contrast agents on left ventricular parameters calculated by a threshold-based software module: does it truly matter? Int J Cardiovasc Imaging 35(9):1683-1689.
   IF: 1.860

5. Csecs I, Czimbalmos C, Suhai FI, Mikle R, Mirzahosseini A, Dohy Z, Szucs A, Kiss AR, Simor T, Toth A, Merkely B, & Vago H (2018) Left and right ventricular parameters corrected with threshold-based quantification method in a normal cohort analyzed by three independent observers with various training-degree. Int J Cardiovasc Imaging 34(7):1127-1133.
   IF: 1.860

6. Czimbalmos C, Csecs I, Polos M, Bartha E, Szucs N, Toth A, Maurovich-Horvat P, Becker D, Sapi Z, Szabolcs Z, Merkely B, & Vago H (2017) Uncommon presentation of a rare tumour - incidental finding in an asymptomatic patient: case report and comprehensive review of the literature on intrapericardial solitary fibrous tumours. BMC Cancer 17(1):612.
   IF 3.288

6. Baranyai T, Giricz Z, Varga ZV, Koncsos G, Lukovic D, Makkos A, Sarkozy M, Pavo N, Jakab A, Czimbalmos C, Vago H, Ruzsa Z, Toth L, Garamvolgyi R, Merkely B, Schulz R, Gyongyosi M, & Ferdinandy P (2017) In vivo MRI and ex vivo histological assessment of the cardioprotection induced by ischemic preconditioning, postconditioning and remote conditioning in a closed-chest porcine model of reperfused acute myocardial infarction: importance of microvasculature. J Transl Med 15(1):67.
   IF: 4.197

7. Maurovich-Horvat P, Suhai FI, Czimbalmos C, Toth A, Becker D, Kiss E, Ferencik M, Hoffmann U, Vago H, & Merkely B (2017) Coronary Artery Manifestation of Ormond Disease: The "Mistletoe Sign". Radiology 282(2):356-360.
   IF 7.469

8. Kiss O, Sydo N, Vargha P, Vago H, Czimbalmos C, Edes E, Zima E, Apponyi G, Merkely G, Sydo T, Becker D, Allison TG, & Merkely B (2016) Detailed heart rate variability analysis in athletes. Clin Auton Res 26(4):245-252.
   IF: 1.276